

ADVANCED SURFACE POLISHING FOR ACCELERATOR TECHNOLOGY USING ION BEAMSZ. Insepov*, J. Norem*, A. Hassanein[#], A.T. Wu[&]

*) Argonne National Laboratory, 9700 South Cass Avenue, Argonne, IL 60439, USA

[#]) Purdue University, 500 Central Drive, West Lafayette, IN 47907, USA[&]) Thomas Jefferson National Accelerator Facility, 12000 Jefferson Avenue, Newport News, VA 23606, USA**ABSTRACT**

Surface erosion problems are common in the development of TeV accelerators, fusion and fission reactors, semiconductor, optical and magnetic storage devices, and Extreme Ultra-Violet (EUV) lithography devices. We have reviewed various erosion mechanisms of ion interactions with the surfaces studied by experiment and computer simulation. Nanoscale surface roughness in *rf*-linacs and contamination cause field emission of electrons, field evaporation of ions and fragments, plasma formation, and lead to high-gradient *rf* vacuum breakdown of electrodes which is a limiting factor in the development of high-gradient *rf* technology for future TeV accelerators. A few mechanisms of nanoscale surface fracture under a high-gradient electric field were developed and will be discussed. A Gas Cluster Ion Beam (GCIB) technology was successfully applied to surface treatment of Cu, Stainless steel, Ti and Nb samples and to Nb *rf*-cavities by using accelerated cluster ion beams of Ar, O₂, N₂, and NF₃, and combinations of them, with accelerating voltages up to 35 kV. DC field emission (dark current) measurements and electron microscopy were used to investigate metal surfaces treated by GCIB. The experimental results showed that GCIB technique can significantly reduce the number of field emitters and also change the structure of the Nb oxide layer on the surface. The RF tests on the GCIB treated Nb *rf*-cavities showed improvement of the quality factor Q at 4.5 K. The superconducting gap was also enhanced by using the oxygen GCIB irradiation exposure. GCIB may become a standard technique to modify and control the oxygen content on the surface and a promising surface treatment technique for Nb SRF cavities in particle accelerators. Computer simulation of bombardment of Nb surfaces with Ar and O₂ clusters by molecular dynamics and phenomenological surface dynamics equations confirms experimental results.

Keywords: *rf* vacuum breakdown mitigation, Gas cluster ion beam; Surface smoothing; molecular dynamics

PACS: 52.80.Vp; 77.22.Jp; 52.40.Kh; 71.15.Pd; 79.20.Rf; 62.50.+p

1. Rf breakdown mitigation in linacs

The behavior of high gradient radio-frequency (*rf*) structures for accelerators is studied in several independent research groups and facilities: Neutrino Factory and Muon Collider Collaboration (NFMCC) [1–5], the International Linear Collider (ILC) [6], and the High Gradient RF Collaboration [7]. Our experimental program studies high gradient *rf* in open and closed-cell cavities in a solenoidal field [1,8], and in the muon ionization cooling experiment (MICE) [9]. The preliminary simulation results were compared our data with the large volume of data [10–13]. The studies of *rf* and DC breakdown have a long history [10–16]. The peak surface field of high field *rf* structures is determined by the tensile strength and parameter β which is a field enhancement factor which depends on the local surface geometry and damage condition and approximately $\beta \approx 200$. In our previous papers, we have outlined a simple model of breakdown based on electrostatic stresses producing fragmentation of highly stressed cavity materials [1,2,8,17]. Atom probe tomography (APT) can be used to get more details in the surface morphology in high electric fields $5 < E < 100$ GV/m [18,19]. The enhancement factor, $\beta = E_{\text{local}}/E_{\text{surf}}$, relates the average surface field and the local field at asperities. DC systems have been shown to break down at an average surface field of about 160 MV/m [10,11], and the local field at asperities of 6–7 GV/m is consistent with the field where tensile

1 stress becomes equal to tensile strength for copper. The primary picture of the frequency dependence of rf
2 breakdown is from Kilpatrick [20]. This scaling law produces roughly the frequency dependence seen in modern
3 data. The model of breakdown triggered by tensile stresses in the material has been discussed elsewhere [1,2,8,17].
4 In this model, fracture of the surface due to electrostatic forces triggers the event. The fragment produced is then
5 heated and ionized by field emitted electron beams to produce a near-surface plasma [21]. The lossy plasma
6 produced then couples the electromagnetic energy of the cavity to the wall, triggering a breakdown event, and
7 ultimately converting most of the stored energy to heat. Experimental evidence for this is obtained from field
8 emitted beams, which show a maximum local surface field at the tips of asperities of $E_{\text{local}} = 7 \text{ GV/m}$ in a wide
9 variety of applications. In APT, small samples of materials are subjected to surface fields from 2–150 GV/m, and the
10 ions produced are identified, permitting computer reconstruction of the material. Long experience with this
11 technology [22] has shown that samples frequently fracture at comparatively low fields (2–10 GV/m) when exposed
12 to high fields. We are actively developing this area by computer simulation [3].

13 There are a number of questions that require more experimental data, however, such as field emission, heating from
14 field emission currents, Coulomb explosion of surface fragments under electron current, creep and fatigue, plasma
15 spots, and the behavior of metals under high fields in general. In addition, how mechanical forces apply in complex
16 systems, at the nanoscale, is not well understood. Adsorbed gas or loosely bound oxides have often been proposed as
17 the trigger for breakdown, assuming that this gas is ionized and produces a plasma. Other mechanisms that have
18 been proposed include plasma spots, field emission, and multipactor. Plasma spots, which have been seen on the
19 surface of a number of cavities, are the basis of a model proposed by Wilson [23], and these predictions have been
20 found useful [24]. Field emission is the most visible result of the operation of high gradient surfaces [21,25].
21 Multipactoring has often been associated with breakdown events [23,26].

22 In our previous paper [3], we proposed a new surface damage mechanism called “cluster field evaporation” where
23 the narrow tips at the cavity surface can easily torn out from the surface in a strong electric gradient and create
24 particles in the rf cavity that can easily be dispersed to smaller parts by the bombardment of field emitted electrons,
25 heated up and be blown via a Coulomb explosion mechanism. We showed that the critical fields $\sim 7 \text{ GV/m}$ of field
26 evaporation of clusters is much lower than those of a single ion ($\sim 20 \text{ GV/m}$) [3]. We are currently working on the
27 development of this mechanism by using atomistic and plasma simulation codes.

28 **2. Surface treatment of SRF cavities by gas cluster ion beam technique (GCIB)**

1 The GCIB technology was developed for surface modifications of semiconductor, metal, insulating surfaces and
2 ion-assisted thin film deposition at the Ion Beam Engineering Experimental Laboratory of Kyoto University by Isao
3 Yamada and co-workers [32-36]. A cluster is an aggregate of atoms or molecules interacting via weak Van-der
4 Waals forces containing from a few hundreds to tens of thousand atoms or molecules and having a few elemental
5 charges that can be produced by an adiabatic expansion of a compressed at a high pressure gas (~15 bar) into a
6 region of high vacuum ($\sim 3 \times 10^{-6}$ bar) [35-37]. The gas cluster ion beams are characterized by a very low energy per
7 atoms that is characteristic for a localized surface effect. A lateral sputtering effect can be a driving force behind the
8 surface smoothing effect [38]. Surface treatment by cluster ions can increase the surface density and can seal
9 vacancy pores on the subsurface region [39]. The clusters are ionized by an electron impacts, extracted by an electric
10 field and filtered by passing them through magnet and/or electrostatic filters and then electrostatically accelerated
11 toward the target. The acceleration voltage is in the range of 5-35 kV and the total ion current of a gas cluster beam
12 can be as high as 1 mA [37]. The cluster beam has a broad distribution of clusters over the cluster sizes. An effort
13 has been made to create a narrow-sized beams by using various size-selection equipment [34,35].

14 GCIB technique was used to modify surfaces of Cu, Nb, Stainless steel (SS), and Ti electrode materials using beams
15 of Ar, N₂, O₂, NF₃+O₂ clusters with accelerating potentials up to 35 kV [40-45]. Highly polished stainless steel
16 electrode material samples for high-field photoelectron guns were obtained from Cornell Wilson Laboratory [41].
17 These surfaces were hand-polished to an average roughness of <1 μm and the surface showed isolated asperities and
18 sharp-edged, ~200-nm-wide scratches produced by the polishing compound. A dramatic reduction in the number of
19 field emission sites have been seen in a scanning field emission microscope (SFEM) on stainless steel and Nb
20 coupons treated with GCIB [42]. Evaluation of irradiated SS and Ti surfaces by using SEM and AFM imaging
21 obtained a significant smoothing effects: a 200-nm-wide polishing scratch marks were greatly polished out.
22 The most striking result was observed on a 150-mm diameter GCIB-treated stainless steel electrode that has shown
23 almost 10^6 times reduce of the dark current and no DC field emission current at high gradients of 20 MV/m [46].
24 The Power Spectral Density (PSD) analysis of the AFM measurements of these surfaces showed that GCIB
25 treatment efficiently removes the irregularities with the sizes in the interval of 0.1-2 μm . Fig. 1a and 1b show AFM
26 image (20 \times 20 μm) of a highly polished stainless steel electrode material before GCIB treatment showing asperities
27 and scratch marks from polishing and after GCIB treatment [41]. Similar results were obtained by treating Ti
28 surfaces.

1 The field emission was measured at the Jefferson Laboratory Large Area Electrode Test Chamber and later on an
2 identical test stand at Cornell Wilson Laboratory. A gradient of over 20 MV/m was reached with no measurable
3 field emission [44]. The processing of this electrode included treatments with O₂ clusters which increased the
4 thickness of surface oxide layer from 1.5 nm to >10 nm and the surface becomes twice as hard compared to the
5 untreated surface [41,42]. The relative contributions of smoothing, oxide thickness and surface hardening to the
6 reduction in field emission are receiving further study [43,44].

7 The Nb SRF samples were supplied by Jefferson Laboratory and treated by GCIB technique at Epion and returned
8 back to JLab for analysis. Field emission was studied by using the Scanning Field Emission microscope (SFEM)
9 [44]. The emitters detected on the Nb surfaces by SFEM can be analyzed by SEM and EDX. Experimental results of
10 a Nb sample treated by GCIB are shown in Fig. 2. The sample was masked into quadrants shown in the figure. The
11 region marked “Unprocessed” were masked during the experiment. “P1” was treated by Ar and “P1+P2” - by Ar and
12 then additionally O₂. “P2” region was treated by O₂ clusters. The triangles in the figures show the locations of the
13 emitters and the height of them are proportional to the emission intensity. Retesting of these samples showed the
14 same result as it is seen in Fig. 2b) [41-44]. Total 23 emitters were found on the untreated portion of the sample and
15 only 3 – on the treated part.

16 The morphology of Nb surfaces treated by GCIB was examined by an atomic force microscope (AFM) and a high
17 precision 3-D profilometer [45]. The average roughness of Nb samples did not correlate with the level of GCIB
18 treatment. Typically the RMS of the treated region is 615 nm over an area of 200×200 μm² as compared with 315
19 nm for the untreated region.

20 A grand challenge is to develop a detailed materials science description of the Nb oxides on the surface of
21 superconducting cavity under extremely high electric and magnetic fields at an atomistic scale. This is absolutely
22 necessary to mitigate and resolve the rf-vacuum breakdown and Q-slope problems [1-3]. Q-slope is a sudden
23 increase in rf losses leading to a decrease of the cavity quality factor Q at a moderate and high accelerating fields.
24 Although a cure for Q-drop exists, consisting of a modest temperature heat treatment, the understanding of its
25 cause(s) is still lacking. The performance of Nb SRF cavities depends critically on the surface top layer of about 50
26 nm thickness. An approximately 6 nm of the top layers are covered by insulating pent-oxide Nb₂O₅. Sub-oxides of
27 metallic nature Nb₂O, Nb_xO, may not be superconducting. These sub-oxides can degrade the RF performance of Nb
28 cavities. One of the major features of GCIB technique is the ability to controllable growth of oxide layers by

1 irradiating metal surfaces with O₂ cluster ions. The GCIB treatment of Nb surface oxide layers was examined via a
2 dynamic SIMS system [45] was employed. Although the mechanisms of pent-oxide are not clear yet, the results
3 show that GCIB treatment makes cleaner surfaces completely eliminating such elements as Na, Ca. GCIB has also
4 converted low Nb-oxides into pent-oxide, increased the amount of oxygen in the interior of Nb by increasing the
5 diffusivity of O [43,44].

6 The Nb SRF single cell cavities treated by GCIB at Epion were tested against their rf performance. O₂ clusters were
7 selected for the initial GCIB treatments on Nb single cell cavities. A cluster ion beam deflector was designed and
8 made before the treatments could be done on a Nb cavity. Two separate tests were conducted on rf-cavities for 1.3
9 GHz and 3.9GHz Nb single cell cavities made at JLab and Fermi Lab. After the GCIB treatment at Epion, the
10 cavities were RF tested at JLab. One of the main gains that GCIB treatment provided was an increase of the
11 superconducting gap for the first cavity. The second test obtained an increase of the quality factor Q₀ [44]. At the
12 same time, a strong multipacting was found due to possible contamination on the treated surface due to improper
13 handling during the operations of assembly and disassembly.

14 **3. Computer simulation in Nb surface treatment by GCIB**

15 To understand the mechanisms associated with the modifications of morphology on Nb (100) surfaces by GCIB
16 treatments, computer simulations through molecular dynamic modeling were employed [47-50]. Ar and O₂ were
17 selected as the species for the GCIB clusters containing 429 molecules or atoms. It was found that heavier GCIB
18 species such as Ar could generate larger and deeper craters than those generated by lighter GCIB species on a Nb
19 surface as shown in Fig. 5. The kinetic energy of Ar was assumed to be 125 eV/atom and that of O₂ was 100
20 eV/molecule. This could explain the results found from the profilometer measurements on the samples treated by
21 NF₃+O₂ as shown in Figs. 5a,b). Smoothing effect by GCIB treatments was demonstrated by modeling a Nb surface
22 containing two types of surface tips with significantly different sizes. One tip was a narrow and tall hill with a
23 typical diameter of a few nm. The other was a wide and short hill having a typical diameter of many tens of nm.
24 Both tips had equal volumes and were schematically shown in Fig. 6. The total modeled area was in the order of
25 10⁶–10⁷ Å², and this area was randomly irradiated by up to 1000 30 keV O₂ clusters. The cluster fluence was in the
26 order of 10³–10⁴ cluster/cell which corresponded to the range of 10¹²–10¹⁵ ion/cm², average cluster sizes of 10³
27 particles, and the total cluster energies was 30 keV. Fig. 6 demonstrates the results of our mesoscale simulations for
28 Nb surface smoothening. The residual roughness is always defined by the geometry of an individual crater and

1 increases with the increase of the total cluster ion energy. The simulation showed that the narrower hill could be
 2 removed by an irradiation dose that was five times lower than that required for the blunt hill. The larger the surface
 3 bump is in the horizontal plane, the higher irradiation dose is needed to completely remove the hill and smooth the
 4 surface. It is known that the narrower hills have a higher chemical potential than those with a larger diameter.
 5 Therefore GCIB surface treatments should remove the narrow hills faster than the wider ones. Computer simulation
 6 suggests that the surface smoothing of Nb is mostly done by physical removal rather than by chemical reaction [49].

7 **4. Plasma model of surface erosion in rf cavity**

8 When a plasma gets into contact with the surface, it causes various physical processes: electron emission, ion
 9 sputtering, thermal evaporation, and unipolar arcing. The latter is the most surface damaging process. The existence
 10 of unipolar arcing was experimentally verified on many tokamak devices [51]. A unipolar arc is developed in a
 11 space near the surface if the sheath potential is sufficiently high and such arc can seriously damage the surface. A
 12 unipolar arc with $kT_e \approx 100$ eV was studied in [52-54] by irradiating a laser beam to a metal surface. A detailed
 13 analysis of the plasma model will be published elsewhere [55]. The near-surface fast expanding laser-produced
 14 plasma with the density of 10^{13} - 10^{21} cm⁻³ was created and about 20,000 unipolar arc and craters were observed on
 15 the stainless steel surface within a few hundred of nanoseconds. The sheath (floating) potential is as follows [52]:

$$\begin{aligned}
 U_f &= (kT_e / 2e) (\ln M_i / 2\pi m_e) \\
 \lambda_D &= (kT_e / 2\pi n e^2)^{1/2}, \\
 E_f &\approx -U_f / \lambda_D,
 \end{aligned}
 \tag{3}$$

17 where U_f and E_f are the sheath potential and electric field, k is the Boltzmann constant, T_e is the electron temperature,
 18 e – elemental charge, M_i is the ion mass, m_e is the electron mass, n – the plasma density, and λ_D is the Debye length.

19 The sheath electric field between the surface and plasma E_f will be added to the average surface field E_{surf} existing in
 20 rf-cavity and this gives $E_{local} \approx 2.4$ GV/m which is close to the critical field of the field evaporation model [3].

21 Electron emission from the surface or a sudden increase of the plasma density reduces the plasma potential, thus
 22 more plasma electrons reach the surface and close up the current loop. It is not clear what is the reason of the initial
 23 breakdown and formation of the cathode spot. It is believed that thin dielectric spots or films (oil, grease) can lead to
 24 enhanced arc formation [51]. We have added a few important elements into the Schwirtzke model: i) Surface
 25 electric field will be much higher in rf linac due to existing acceleration field [1]; ii) the local field enhancement
 26 factor $\beta \sim 200$ [2,17]; iii) Field evaporation of the fragments of the tips into the rf cavity space [3,50]; iv) Coulomb

1 explosion of the fragments that would lead to a non-linear growth of the local plasma density due to local heat
2 release and that triggers a ring-shape opposite electron current back to the surface [47]; v) the arc in rf linac cavity
3 is in fact not completely unipolar but has a significant bipolar component which can be verified by experiments with
4 rf cavity rf tests [1,17].

5 We study the interactions between the cavity rf parameters and the cavity operation, in the combined results of an
6 experimental program at Fermilab [1-3,8,17], some modeling and initial studies of the material science of surfaces
7 under high electric stress. This effort should explain how multi-cell structures cannot achieve the operating fields of
8 single cell structures, and how structures with long pulses generally require lower fields than those with short pulses.
9 The model describes the breakdown process in terms of: 1) fracture of a small fragment, 2) ionization of this
10 fragment, 3) formation of a stable plasma, somewhat similar to a unipolar arc, and 4) the time development of this
11 plasma to the point where it produces sufficient electrons that can short out the cavity. We believe that effects such
12 as Coulomb explosions could be used to describe both the breakup of fragments in a field emission beam, as well as
13 the breakup of the original surface. This model can produce a detailed picture of the operation of rf structures at their
14 operating limits. The assumptions above can be used to produce predictions of an extremely large range of
15 parameters. We hope this work will be useful in improving the understanding of these phenomena and in suggesting
16 experiments that can increase the precision of the model. One conclusion of this effort is that producing and
17 maintaining the smoothest possible surfaces is of primary importance. Thus all techniques that can be used to
18 smooth the interior surfaces of all rf structures may be the best way to insure the highest operating fields. A natural
19 application of this model is to generate scaling laws for maximum gradient as a function of frequency, to compare
20 with the well-known Kilpatrick limit [17]. The geometry, pulse length, tolerable breakdown rate, power systems and
21 controls can have a significant influence both on the structure and the model. Nevertheless, the logarithmic
22 dependence of the maximum gradient is consistent with experimental data.

23 **SUMMARY**

24 *RF* vacuum breakdown models were discussed and a new model was examined. GCIB processing is effective at
25 smoothing roughness of size scales less than 1-2 μ m, and we have shown efficient etching of isolated asperities 300
26 nm in diameter and 35 nm in height. Thus GCIB processing is uniquely capable of smoothing roughness of the scale
27 of the field emitters that have been identified on Cu and stainless steel electrodes. There is also strong evidence that
28 GCIB can significantly suppress field emitters on Nb SRF cavity surfaces. Achieving a 20 MV/m gradient without

1 appreciable field emission is exceptional result of GCIB treatment of Nb cavity. Theoretical study by computer
 2 simulation revealed that narrower and tall hills on Nb surfaces could be removed by an irradiation dose that was five
 3 times lower than that required for blunt and short hills. The larger a surface hill was in the horizontal plane, the
 4 higher irradiation dose was needed to completely remove the hill and smooth the surface. It was found that, in
 5 general, GCIB treated Nb surfaces were cleaner than the untreated surface. O₂ GCIB treatments introduced
 6 interstitial O atoms to the top oxide layer on Nb surfaces and increased its thickness too. On the other hand, NF₃
 7 GCIB treatments reduced the thickness of the top oxide layer. We found no evidence that N₂ GCIB treatments could
 8 produce the desirable NbN on Nb surfaces.

9 *Acknowledgments*

10 This work was supported by the U.S. Dept. of Energy under Contract DE-AC02-06CH11357.

11
 12 **REFERENCES**

- 13 [1] J. Norem, V. Wu, A. Moretti, M. Popovic, Z. Qian, L. Ducas, Y. Torun, and N. Solomey, Phys. Rev. ST Accel.
 14 Beams **6**, 072001 (2003).
 15 [2] J. Norem, Z. Insepov, and I. Konkashbaev, Nucl. Instrum. Methods Phys. Res., Sect. A **537**, 510 (2005).
 16 [3] Z. Insepov, J. H. Norem, and A. Hassanein, Phys. Rev. ST Accel. Beams **7**, 122001 (2004).
 17 [4] Feasibility Study-II of a Muon Based Neutrino Source, edited by S. Ozaki, R. Palmer, M. Zisman, and J.
 18 Gallardo
 19 BNL-52623 (2001), <http://www.cap.bnl.gov/mumu/studyii/>.
 20 [5] M. M. Alsharo at al, Phys. Rev. ST Accel. Beams **6**, 081001 (2003).
 21 [6] <http://www.linearcollider.org/cms/>
 22 [7] <http://www.slac.stanford.edu/grp/ara/HGCollab/HomePage/HGHome.htm>
 23 [8] A. Moretti, Z. Qian, J. Norem, Y. Torun D. Li, and M. Zisman, Phys. Rev. ST Accel. Beams **8**, 072001 (2005).
 24 [9] <http://hep04.phys.iit.edu/cooldemo/>.
 25 [10] R. F. Earhart, Philos. Mag. **1**, 147 (1901).
 26 [11] G. M. Hobbs, Philos. Mag. **10**, 617 (1905).
 27 [12] Lord Kelvin, Philos. Mag. **8**, 534 (1904); also Voltaic Theory, Radioactivity, Electrons, Navigation and Tides,
 28 Miscellaneous, Mathematical and Physical Papers (Cambridge University Press, Cambridge, England, 1911), Vol.
 29 VI, p. 211.
 30 [13] Handbook of Vacuum Arc Science and Technology, edited by R. L. Boxman, P. J. Martin, and D. M. Sanders
 31 (Noyes Publications, Park Ridge, NJ, 1995).
 32 [14] D. Alpert, D. A. Lee, E. M. Lyman, and H. E. Tomaschke, J. Vac. Sci. Technol. **1**, 35 (1964).
 33 [15] R. L. Kustom, J. Appl. Phys. **41**, 3256 (1970).
 34 [16] L. L. Laurent, Ph.D. thesis, University of California, Davis, 2002.
 35 [17] A. Hassanein, Z. Insepov, J. Norem et al, Effects of surface damage on rf cavity operation, Phys. Rev. STAB **9**,
 36 062001 (2006).
 37 [18] J. Norem, P. Bauer, J. Sebastian, and D. N. Seidman, Proceedings of PAC05, Knoxville, TN, 2005, p. 612.
 38 [19] M. K. Miller, Atom Probe Tomography (Kluwer Academic/Plenum Publishers, New York, 2000).
 39 [20] W. D. Kilpatrick, Rev. Sci. Instrum. **28**, 824 (1957).
 40 [21] R.W. Wood, Phys. Rev. **5**, 1 (1897).
 41 [22] P. J. Birdseye, D. A. Smith, Surf. Sci. **23**, 198 (1970).
 42 [23] P. Wilson, Proceedings of LINAC 2004, Lubeck, Germany, 2004, p. 189.
 43 [24] V. A. Dolgashev and S. G. Tantawi, RF Breakdown in X Band Waveguides, Proceedings of EPAC 2002, Paris,
 44 2002, p. 2139.
 45 [25] W.W. Dolan, W. P. Dyke, and J. K. Trolan, Phys. Rev. **91**, 1054 (1953).
 46 [26] R. Kishek *et al.*, Phys. Plasmas **5**, 2120 (1998).

- 1 [27] S. Yamaguchi, High Gradient RF Workshop, Argonne, 2003, [http:// gate.hep.anl.gov/rf/](http://gate.hep.anl.gov/rf/).
2 [28] H. H. Braun, S. Dobert, I. Wilson, and W. Wuensch, Phys. Rev. Lett. **90**, 224801 (2003).
3 [29] U.S. Workshop on High Gradient RF for Multi-TeV Linear Colliders, SLAC, 2005.
4 [30] J. Ozelis (private communication).
5 [31] M. Kelly (private communication).
6 [32]. I. Yamada, Proc. 14th Symp. on Ion Source and Ion-Assist. Techn., Tokyo, Japan (1991) p. 227.
7 [33]. I. Yamada, Rad. Eff. Def. in Sol. 124 (1992) 69
8 [34] I. Yamada, N. Toyoda, Nucl. Instr. Meth. in Phys. Res. B 241 (2005) 589–593.
9 [35] I. Yamada, N. Toyoda, Nucl. Instr. Meth. in Phys. Res. B 232 (2005) 195–199.
10 [36]. I. Yamada and N. Toyoda, Surface & Coating Technology, 201 (2007) 8579.
11 [37]. D.R. Swenson, Nucl. Instr. Meth. B 222 (2004) 61.
12 [38] Z. Insepov, M. Sosnowski, I. Yamada, Trans. Mat. Res. Soc. Jpn 17 (1994) pp.111-118.
13 [39] H. Haberland, Z. Insepov and M. Moseler, Phys. Rev. B 51, (1995) p.11601.
14 [40] D.R. Swenson, E. Degenkolb, Z. Insepov, L. Laurent, G. Scheitrum, NIMB B241 (2005) 641–644.
15 [41] D.R. Swenson, E. Degenkolb, Z. Insepov, Physica C 441 (2006) 75-78.
16 [42]. D.R. Swenson, A.T. Wu, E. Degenkolb, Z. Insepov, CP877, Adv. Accel. Concepts: 12th Workshop, ed. M.
17 Conde and C. Eyberger, AIP (2006).
18 [43]. D.R. Swenson, A.T. Wu, E. Degenkolb, Z. Insepov, Nucl. Instr. Meth. in Phys. Res. B 261 (2007) 630–633.
19 [44] A.T. Wu et al, Invited contribution to a chapter of the book "Particle Accelerators: Research, Technology, and
20 Applications" by NOVA Science Publishers (2008). Officially accepted for publication on Aug. 4, 2008.
21 [45]. A.T. Wu, Proceedings of the 11th SRF Workshop, Germany, 2003 ThP13
22 [46] C.K. Sinclair, private communication.
23 [47] Z. Insepov, A. Hassanein, D. Swenson, Physica C 441 (2006) 114–117.
24 [48] Z. Insepov, J. Norem, D.R. Swenson, A. Hassanein, M. Terasawa, Nucl. Instr. Meth. in Phys. Res. B 258
25 (2007) 172–177.
26 [49] Z. Insepov, A. Hassanein, J. Norem, D.R. Swenson, Nucl. Instr. Meth. in Phys. Res. B 261 (2007) 664–668.
27 [50] Z. Insepov, J. Norem, D.R. Swenson, A. Hassanein, Vacuum 82 (2008) 872–879.
28 [51] G.M. McCracken, J. Nucl. Mater. 93/94 (1980) 3.
29 [52] F.R. Schwirzke, R.J. Taylor, J. Nucl. Mater. 93 & 94 (1980) 780-784.
30 [53] F.R. Schwirzke, J. Nucl. Mater. 128 & 129 (1984) 609-612.
31 [54] F.R. Schwirzke, IEEE Trans. Plasma Sci. 19 (1991) 690-696.
32 [55] Z. Insepov, J. Norem, A. Bross, A. Moretti, Z. Qian, Y. Torun, D. Huang, S. Veitzer, Paper in preparation.
33
34
35
36
37
38
39
40
41
42
43
44
45
46

1
2
3
4
5
6
7

8 The submitted manuscript has been created by UChicago Argonne, LLC, Operator of Argonne National Laboratory
9 ("Argonne"). Argonne, a U.S. Dept. of Energy Office of Science laboratory, is operated under Contract No. DE-
10 AC02-06CH11357. The U.S. Government retains for itself, and others acting on its behalf, a paid-up nonexclusive,
11 irrevocable worldwide license in said article to reproduce, prepare derivative works, distribute copies to the public,
12 and perform publicly and display publicly, by or on behalf of the Government.

1
2
3
4
5
6
7
8
9
10
11
12
13
14
15
16
17
18
19
20
21
22
23
24
25
26
27
28
29
30
31
32
33
34
35
36
37

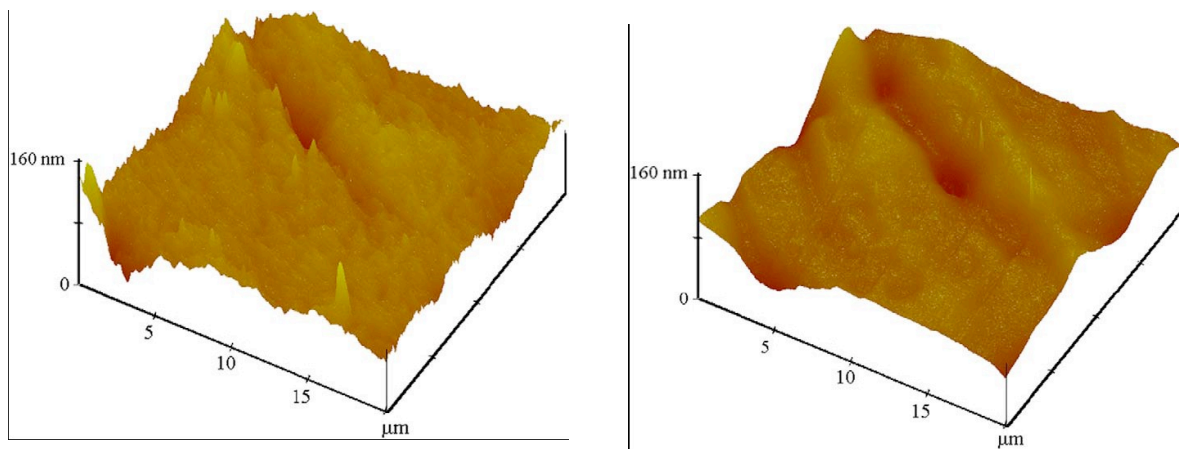


Fig. 1. a) AFM image ($20 \times 20 \mu\text{m}$) of highly polished stainless steel electrode material before GCIB treatment showing asperities and scratch marks from polishing. The vertical scale is 120 nm/division. b). AFM image after GCIB treatment (from [41]).

1
2
3
4
5
6
7
8
9
10
11
12
13
14
15
16
17
18
19
20
21
22
23
24
25
26
27
28
29
30
31
32
33
34
35
36
37
38
39
40
41

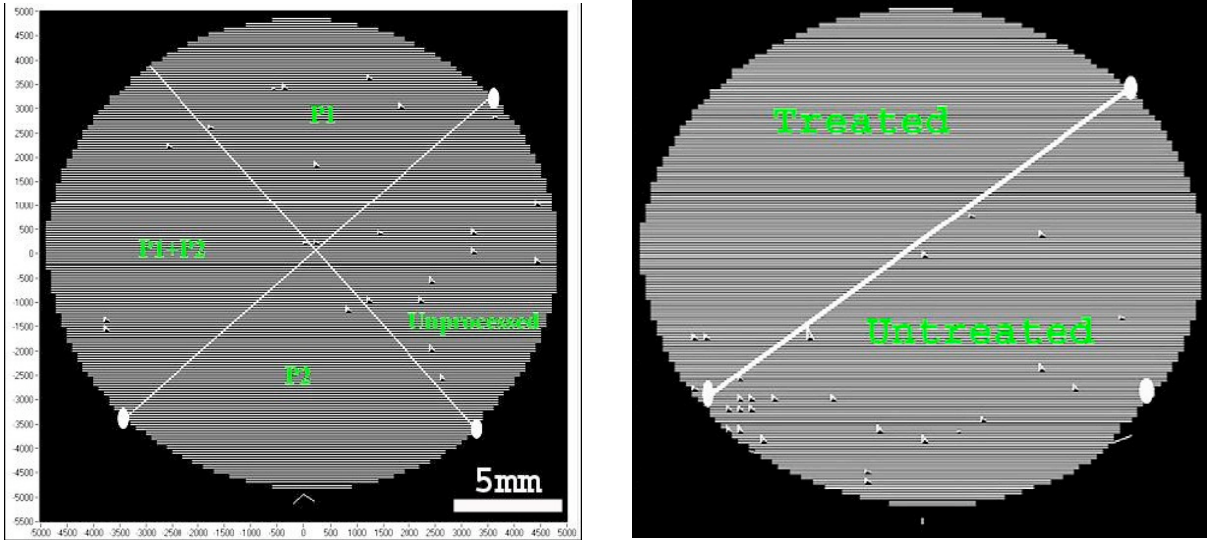


Fig. 2. a): SFEM plot of field emitters on the surface of a BCP treated Nb coupon. The sample was masked into equal quadrants for treatments with Ar and/or O₂ GCIB or not treated as designated in the figure; b) SFEM plot of field emitters on the surface of a BCP treated Nb coupon. Half of the coupon was treated with O₂ GCIB. (from [43])

1
2
3
4
5
6
7
8
9
10
11
12
13
14
15
16
17
18
19
20
21
22
23
24
25
26
27
28
29
30
31
32
33
34
35
36
37
38
39
40
41
42
43
44
45
46
47

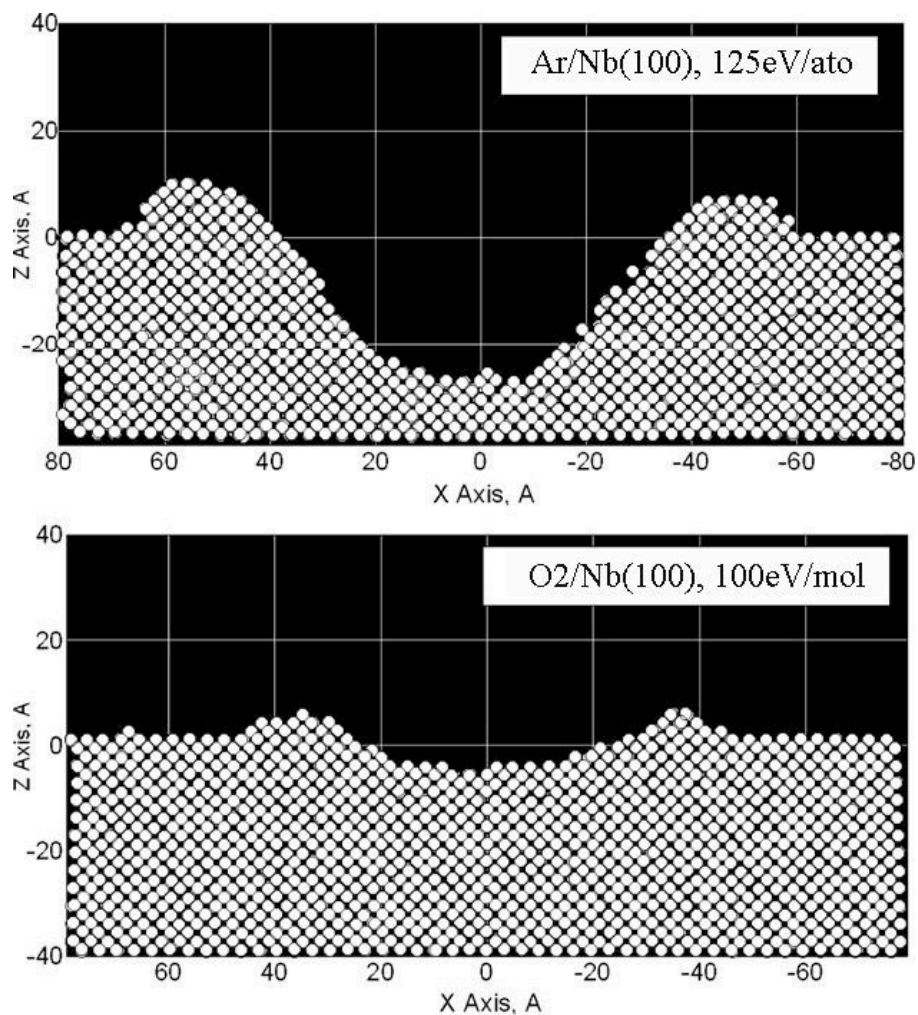


Fig. 3: Craters formed on the surface of (100) Nb treated with a) clusters of 429 Ar at 125 eV/atom, and b) clusters of 429 O₂ at 100 eV/molecule, as calculated by computer simulation via molecular dynamics. (from [43])

1
2
3
4
5
6
7
8
9
10
11
12
13
14
15
16
17
18
19
20
21
22
23
24
25
26
27
28
29
30
31
32
33
34
35
36
37
38
39
40
41
42
43
44
45
46
47
48
49
50
51
52
53
54
55

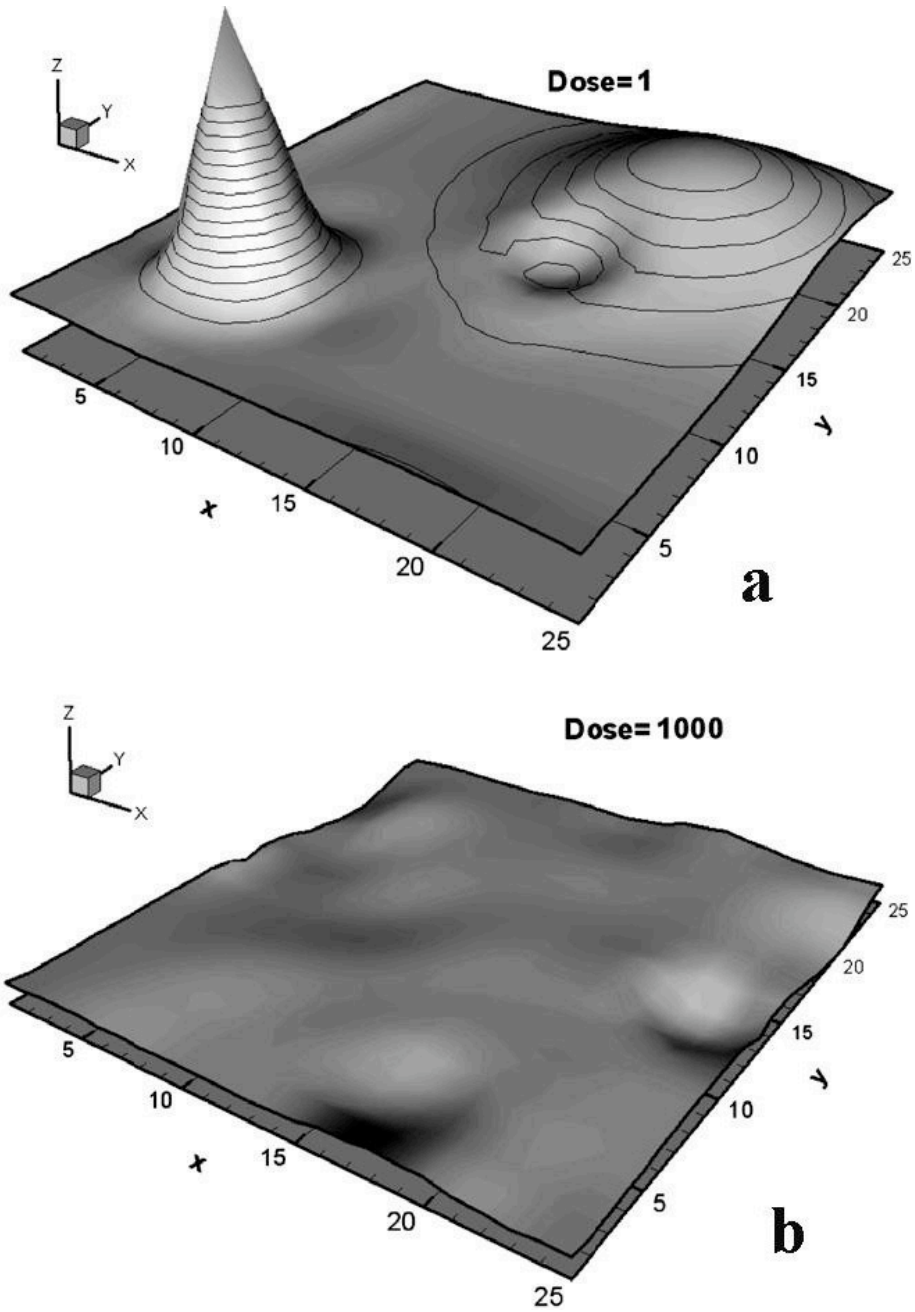


Fig. 4. Results of mesoscale modeling of a Nb surface irradiated by O_2 cluster ion beam at a dose of 10^{13} ions/cm². The cluster energy was 30 KeV and the cluster size was about 3000 oxygen molecules in a cluster. The surface contained two types of features: narrow and tall and wide and short (represented in a)).